

DETRAC: A New Benchmark and Protocol for Multi-Object Tracking

Longyin Wen¹, Dawei Du^{1,2}, Zhaowei Cai³, Zhen Lei⁴, Ming-Ching Chang¹,
Honggang Qi^{1,2}, Jongwoo Lim⁵, Ming-Hsuan Yang⁶, Siwei Lyu¹

¹ Computer Science Department, University at Albany, SUNY

² School of Computer and Control Engineering, UCAS

³ Department of Electrical and Computer Engineering, UCSD

⁴ National Laboratory of Pattern Recognition, CASIA

⁵ Division of Computer Science & Engineering, Hanyang University

⁶ Electrical Engineering and Computer Science, UCM

Abstract

In recent years, most effective multi-object tracking (MOT) methods are based on the tracking-by-detection framework. Existing performance evaluations of MOT methods usually separate the target association step from the object detection step by using the same object detection results for comparisons. In this work, we perform a comprehensive quantitative study on the effect of object detection accuracy to the overall MOT performance. This is based on a new large-scale DETection and tRACKing (DETRAC) benchmark dataset. The DETRAC benchmark dataset consists of 100 challenging video sequences captured from real-world traffic scenes (over 140 thousand frames and 1.2 million labeled bounding boxes of objects) for both object detection and MOT. We evaluate complete MOT systems constructed from combinations of state-of-the-art target association methods and object detection schemes. Our analysis shows the complex effects of object detection accuracy on MOT performance. Based on these observations, we propose new evaluation tools and metrics for MOT systems that consider both object detection and target association for comprehensive analysis.

1. Introduction

Multiple object tracking (MOT), which aims to extract trajectories of multiple moving objects in a video sequence, is a crucial step in understanding and analyzing video sequences. A robust and reliable MOT system is the basis for a wide range of practical applications ranging from video surveillance and autonomous driving to sports video analysis. To date, most effective MOT approaches, e.g., [41, 6, 7, 24, 29, 39, 22, 37, 11], follow the *tracking-by-detection* paradigm, which entails an *object detection*

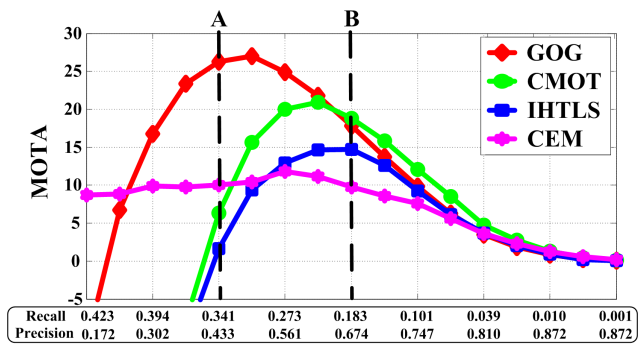


Figure 1: Precision vs. recall vs. multi-object tracking accuracy (PR-MOTA) curves of four different MOT methods provided by the DPM [18] object detection algorithm with four different target association methods: GOG [33], CEM [2], CMOT [4], and IHTLS [37] in the DETRAC dataset. The x -axis corresponds to different precision/recall scores of the DPM detector obtained by varying the detection score threshold. The y -axis is the MOTA score of the MOT methods [33, 2, 4, 37]. Note that with different object detections, highlighted by the two dashed lines A and B, the relative rankings of different MOT methods can vary significantly.

step to find target locations in each video frame (usually in the form of their bounding boxes), and a *target association* step that generates target trajectories by connecting detected locations corresponding to the same target across video frames¹.

Despite significant advances in recent years, considerably less effort has been made to large-scale performance evaluation on MOT methods. We note that there are some benchmark studies of the state-of-the-art object detection methods [17, 14, 20, 34]. Similar efforts for target association methods [9, 5, 20, 28, 26] have been made within the context of MOT, which have shown the effect of various aspects of tracking performance, such as appearance

¹While numerous methods refer the association step as tracking, in this work we make the distinction and the relation can be considered as tracking = detection + association, i.e., the complete MOT system.

ambiguity among targets and occlusions, and provide important information to understand MOT methods. Furthermore, the recent study [28] has indicated the importance of ground truth annotation and evaluation metrics in understanding and analyzing MOT methods.

However, existing performance evaluations of MOT methods usually separate the target association step from the object detection step by using the same object detection results as input for analysis. While this evaluation strategy is widely adopted in the current literature and has yielded useful insights on the MOT methods, it is often insufficient to fully analyze the complete MOT systems (see Figure 1). In particular, it is important to understand the effect of detection accuracy to the overall MOT performance. However, this can only be revealed in a comprehensive quantitative study of the object detection and target association steps *jointly*.

In this work, we perform a comprehensive quantitative study on the effect of object detection accuracy to the overall MOT performance. This is based on a new large-scale MOT benchmark dataset, namely the DETection and tRACKing (DETRAC) dataset. The DETRAC dataset includes 100 challenging video sequences corresponding to more than 140 thousand frames of real-world traffic scenes. These video sequences are manually annotated with more than 1.2 million labeled bounding boxes of vehicles. To the best of our knowledge, this is the largest and most thoroughly annotated MOT evaluation dataset to date (see Table 1 for a detailed comparison with other benchmark datasets), and it poses new challenges for the state-of-the-art object detection and MOT algorithms. We benchmark complete MOT systems constructed from combinations of six target association schemes [2, 33, 3, 12, 37, 4] and four object detection methods [18, 13, 21, 8].

The extensive quantitative benchmark analysis from this work provides interesting and previously unnoticed observations. In particular, previous MOT evaluations use fixed object detections to compare different target association methods, but our experiment results (see Figure 10) show that the relative rankings of target association methods vary significantly with different settings of object detections. Furthermore, some target association methods perform more robustly over different object detection qualities than other association methods. As such, using a fixed set of object detections for evaluation does not reveal the full behavior of the subsequent target association step, and can lead to biased comparisons.

Based on these insights obtained from the benchmark study using the DETRAC dataset, we propose a new evaluation protocol with two new metrics for MOT systems. The proposed DETRAC evaluation protocol considers object detection and target association in tandem. Specifically, we advocate to evaluate MOT performance using the joint

Table 1: Summary of existing object detection or tracking datasets. First six columns: number of training/testing data ($1k = 10^3$) including number of images containing at least one object, number of object tracks, and number of unique object bounding boxes. Final columns: additional properties of each dataset. “D” : detection task, “T” : tracking task, “P” : target object is pedestrian, and “C” : target object is vehicle.

Dataset	Training			Testing			Properties						
	# Frames	Tracks	Boxes	# Frames	Tracks	Boxes	Color imgs.	Video seqs.	Task	Object	Multi. weat.	Occl. labels	Publication
MIT-Ped [32]	924	-	924	123	-	123	✓		D	P			2000
MIT-Car [32]	1.03k	-	1.03k	90	-	90	✓		D	C			2000
INRIA [10]	1.2k	-	1.2k	741	-	566	✓		D	P			2005
ETH [16]	490	-	1.6k	1.8k	-	9.4k	✓	✓	D	P			2007
NICTA [31]	-	-	18.7k	-	-	6.9k	✓		D	P			2008
DDB [15]	-	-	15.6k	21.8k	-	56.5k	✓	✓	D	P			2009
Caltech [14]	67k	-	192k	65k	-	155k	✓	✓	D	P		✓	2012
CUHK [30]	-	-	-	1.06k	-	-	✓		D	P			2012
KAIST [23]	50.2k	-	41.5k	45.1k	-	44.7k	✓	✓	D	P	✓	✓	2015
KITTI-MOD [20]	7.48k	-	40.6k	7.52k	-	39.7k	✓	✓	D	P,C		✓	2014
BU-TIV [38]	-	-	-	6556	-	-	✓	✓	T	P,C			2014
MOT [26]	5.5k	500	39.9k	5.8k	721	61k	✓	✓	T	P	✓		2015
TUD [1]	610	-	610	451	31	2.6k	✓	✓	D,T	P			2008
PETS2009 [19]	-	-	-	1.5k	106	18.5k	✓	✓	D,T	P	✓		2009
KITTI-MOT [20]	8k	-	-	11k	-	-	✓	✓	T	C		✓	2014
DETRAC	84k	5.9k	578k	56k	2.3k	632k	✓	✓	D,T	C	✓	✓	2015

*precision vs. recall vs. multi-object tracking accuracy (PR-MOTA) curve*², and peak PR-MOTA as well as ensemble PR-MOTA scores as two new evaluation metrics. A recent work [35] also addresses the issue of MOT performance evaluation with fixed detection results. Similar to our work, this work reveals the inadequacy of using fixed detection inputs adopted in the current MOT evaluation strategy, and suggests to study target association methods by using multiple noise perturbed detection results from the ground truth annotations. However, evaluating with artificially perturbed detections do not reflect the behavior of an object detector in practice. In contrast, our analysis is based on the actual outputs of the state-of-the-art object detectors with full range of their precision-recall rates. From this perspective, our analysis and MOT evaluation strategy provide a closer description of how a complete MOT system *in the wild* performs.

The main contributions of this work are summarized as follows.

- We present a large-scale DETRAC dataset for MOT evaluation, which is distinctly different from existing database in terms of data volume, annotation quantity and quality, and challenge levels (see Table 1).
- We propose new evaluation protocol and metrics for MOT systems by considering object detection and tar-

²Multi-Object Tracking Accuracy (MOTA) [36] is the most widely used metric to evaluate target association performance, which combines three sources of errors into a single number.



Figure 2: Screenshots of annotated frames in each sequence of the DETRAC datasets. The first six rows present the DETRAC-train set and last four rows present the DETRAC-test set. Red bounding boxes are the areas of the annotated target objects. Different numbers represent different targets. Black opaque regions are ignored in the benchmark as general backgrounds. This figure is better view with the electronic copy and zoomed in for details.

get association steps jointly³.

- Based on the DETRAC dataset and evaluation protocol, we perform comprehensive performance evaluations of complete MOT systems by combining state-of-the-art object detection and target association algorithms.
- Our experimental results reveal the complex effect of object detection and target association accuracy to the overall performance MOT systems.

2. DETRAC Benchmark

2.1. Data Collection and Annotation

The DETRAC dataset consists of 100 video sequences, which are selected from over 10 hours of videos taken with a Cannon EOS 550D camera at 27 different various locations, representing various common traffic types and conditions including urban highway, traffic crossings and T-junctions. The videos are recorded at 25 frames per seconds (fps), with the JPEG image resolution of 960×540 pixels. There are more than 140 thousand frames in the DETRAC dataset and

³All the DETRAC datasets, source codes of our evaluation platform, as well as the codes of object detection and association algorithms, will be made publicly available on the website <http://detrac-db.rit.albany.edu> to facilitate large scale performance evaluation.

8, 250 vehicles that are manually annotated, leading to a total of 1.21 million labeled bounding boxes of objects. We also annotate several attributes on the bounding-box, frame and sequence levels:

- **Vehicle category.** We annotated four types of vehicles as, *i.e.*, *car* (62.75% in training and 23.77% in testing), *bus* (1.28% in training and 2.41% in testing), *van* (7.39% in training and 1.49% in testing), and *others* (0.52% in training and 0.38% in testing). The distribution of vehicle category is shown in Figure 4(a).
- **Weather.** We considered four categories of weather conditions, *i.e.*, *cloudy* (19% in training and 11% in testing), *night* (16% in training and 12% in testing), *sunny* (15% in training and 8% in testing), and *rainy* (10% in training and 9% in testing). The distribution of the weather attribute is presented in Figure 4(b).
- **Truncation ratio.** Truncation indicates some parts of the vehicle is outside of the frame. We plot the distribution of vehicle truncation rate in Figure 4(c).
- **Orientation.** We define the vehicle orientation as the angle between the image vertical axis and the central axis of the vehicle determined by its motion vector, which belongs to the interval $[0^\circ, 360^\circ]$. The orientation attribute describes the views of the vehicles in the video (*e.g.*, frontal, side, rear, etc). The distribution of

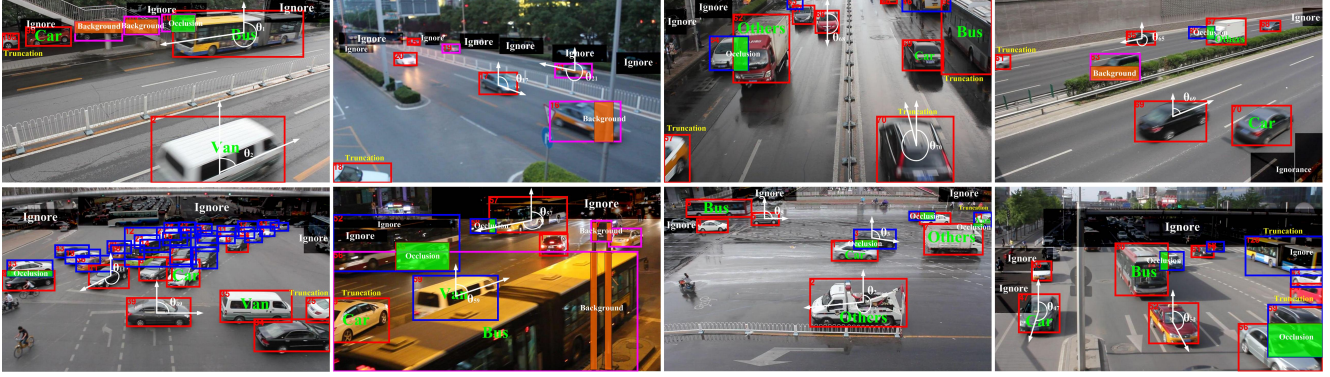


Figure 3: Examples of annotated frames in the DETRAC datasets. Colors of the boundary of the bounding boxes reflect the occlusion property, as fully visible (red), partially occluded by other vehicles (blue), or partially occluded by background (pink). Black opaque regions are ignored in the benchmark as general backgrounds, green opaque regions are areas occluded by other vehicles and orange opaque regions are areas occluded by background. We use highlighted arrows over some vehicles to represent their orientation angles. This figure is better view with the electronic copy and zoomed in for details.

orientation is presented in Figure 4(d).

- **Occlusion ratio.** We use the fraction of vehicle bounding box being occluded to define the occlusion. Figure 4(e) shows the distribution of the occlusion ratio.

We also collected representative statistics over these video frames to facilitate their usage.

- **Vehicle density.** We use the number of vehicles in each frame to describe the vehicle density. Figure 4(f) gives the distribution of vehicle density in the dataset.
- **Scale.** We define the scale of the annotated vehicle bounding boxes as the square root of their area in pixels. The distribution of vehicle scale in the dataset is presented in Figure 4(g).
- **Aspect ratio.** We define the vehicle aspect ratio as the vehicle width divided by height. Figure 4(h) presents the distribution of vehicle aspect ratio in the dataset.
- **Speed.** We use the average speed in pixel per-frame of the vehicle on the image plane to be the vehicle speed. The distribution of the vehicles' speed in the dataset are shown in Figure 4(i).
- **Trajectory Length.** The trajectory length of vehicle is an important characteristic in the dataset. The distribution of target trajectory length is presented in Figure 4(j).

In Figure 2 and Figure 3, we present the screenshots of annotated frames in each sequence in the DETRAC datasets, and several examples of fully annotated video frames with detail attributes, respectively.

The DETRAC dataset is divided into training (DETRAC-train) and testing (DETRAC-test) sets, with 60 and 40 sequences, respectively. We deliberately select training videos that are taken at different locations from the testing videos, but ensure the training and testing videos share similar traffic conditions and attributes. Such a setting reduces the chance of the object detector or MOT method to overfit to particular scenarios, while still ensures

Table 2: Evaluated object detection and target association algorithms.

Methods	Description
DPM [18]	The mixtures of multiscale deformable part models for object detection trained by a latent SVM algorithm.
ACF [13]	A fast feature pyramids used for object detection by an approximate extrapolation strategy, which is inexpensive as compared to direct multi-resolution image feature computation.
R-CNN [21]	A regions with convolutional neural network (CNN) features applied to bottom-up region proposals to localize and segment objects, and a supervised pre-training presented for an auxiliary task followed by domain-specific fine-tuning.
CompACT [8]	A new cascade procedure by formulating cascade learning as the Lagrangian optimization of a risk of accuracy and complexity.
CEM [2]	Target association formulated as minimization of a continuous energy function and an optimization algorithm presented to determine strong local minimal.
GOG [33]	A highly efficient network flow based optimization method used to complete target association, which is solved by a min-cost flow algorithm.
DCT [3]	Target association formulated as a discrete-continuous optimization problem, where data association is performed using discrete optimization and trajectory estimation is posed as a continuous fitting problem.
IHTLS [12]	Target association formulated as a generalized linear assignment of tracklets incrementally based on the motion dynamics.
H ² T [37]	Target association formulated as a hierarchical dense neighborhood searching problem on the hypergraph, where the high-order similarities among tracklets are considered.
CMOT [4]	Target association task completed based on the tracklet confidence using the detectability and continuity of a tracklet.

generalization from training to testing phases.

2.2. Benchmarked Algorithms

We evaluate performance of different MOT systems on the DETRAC dataset, which are constructed by the combinations of four state-of-the-art object detection algorithms and six target association algorithms⁴.

Object detection. We evaluate the following four state-of-the-art object detection algorithms including DPM [18], ACF [13], R-CNN [21], and CompACT [8]. We retrain these methods on the DETRAC-train dataset and evalu-

⁴All source codes of the object detection and target association algorithms are publicly available or provided by the authors.

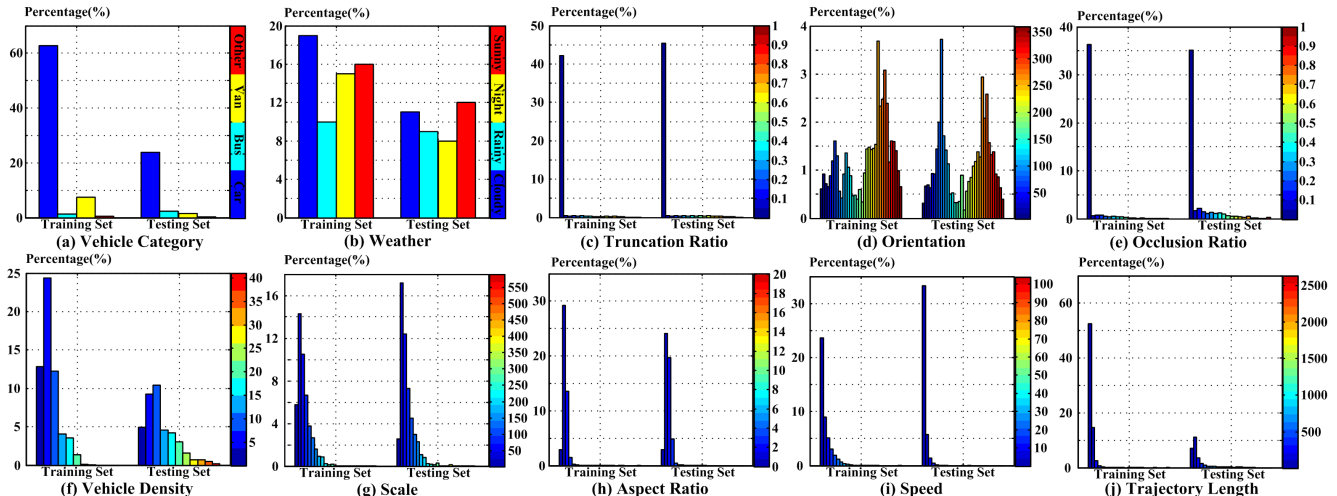


Figure 4: Ten different attribute statistics of the DETRAC benchmark. This figure is better view with the electronic copy and zoomed in for details.

ate their performance on the DETRAC-test set. The DPM method is trained using a mixture of 3 star models and each of which have 2 latent orientations. The ACF cascade uses 2048 decision trees of depth 4. For the CompACT scheme, we train a cascade of 2048 decision trees of depth 4, using all handcrafted features in [8] except CNN features. For the ACF and CompACT methods, the template size is set to 64×64 . To detect vehicles with different aspect ratios, the original images are resized to six different aspect ratios before detection happens, such that only a single model is needed. A bounding box regression model based on the ACF features is trained for the ACF and CompACT detectors to get better detection performance. For the R-CNN algorithm, we fine-tune the AlexNet [25] on the DETRAC-train dataset. Instead of using selective search to generate proposal, the output bounding boxes of the ACF method are warped to 227×227 patches and then input into the R-CNN framework for classification. The bounding box regression in the R-CNN method is not used. The positive samples are all types of vehicles from the DETRAC-train dataset, while the KITTI-MOD dataset [20] is included for hard negative mining. The minimum size of the detected object is set as 25×25 for all detectors.

Target association. We evaluate six state-of-the-art target association algorithms based on the object detection including GOG [33], CEM [2], DCT [3], IHTLS [12], H²T [37], and CMOT [4]. We use the DETRAC-train dataset to determine the parameters for these methods, and the DETRAC-test set for evaluation.

2.3. Comparison to Existing Benchmarks

Object detection benchmarks: Several benchmarks exist for object detections, *e.g.*, Pascal VOC [17], ImageNet [34], Caltech [14], KITTI-MOD [20], and Multispectral Pedestrian dataset [23]. However, the main focus of these bench-

marks is object detection, and they provide useful baseline results when detectors are incorporated in MOT systems.

MOT benchmarks: Several MOT tracking benchmarks have also been collected for evaluating the state-of-the-art target association methods. Some of the most widely used MOT benchmarks are the PETS2009 [19], KITTI-MOT [20] and MOTChallenge [26]. The PETS2009 dataset is a large crowd dataset that focuses on multi-pedestrian tracking and counting. The KITTI-MOT benchmark is a multi-vehicle tracking dataset, taken from a moving vehicle with the viewpoint of the driver. The KITTI-MOT and KITTI-MOD benchmarks are for object tracking and detection separately. The MOTChallenge aims to provide a unified dataset, platform, and evaluation protocol for existing MOT methods. It includes a dataset of 22 video sequences mostly from surveillance cameras with the tracking targets of interest being pedestrians. In addition, it also provides an open system where new datasets and MOT methods can be incorporated in a *plug-n-play* manner. Compared to existing MOT benchmarks, the DETRAC benchmark focuses on vehicle surveillance applications, with a significant larger quantity of video frames, annotated bounding boxes and attributes. Table 1 presents a summary of the differences between existing and proposed DETRAC benchmarks in various aspects.

3. DETRAC MOT Evaluation Protocol

As discussed in Section 1, existing MOT evaluation protocols that use the same set of object detections as input are not adequate to understand overall MOT system performance. In this section, we introduce a new MOT evaluation protocol, DETRAC MOT, that considers object detection and target association jointly.

3.1. Basic Evaluation Metrics

Evaluation metrics for object detection. Similar to [20], we use the *precision vs. recall* (PR) curve for object detection. The PR curve is generated by tuning the threshold of an object detector to generate different precision and recall values. Per-frame detection evaluation is performed as in the PASCAL VOC [17], with the hit/miss threshold of the overlap between a detection bounding box and a ground truth bounding box set to 0.7.

Evaluation metrics for target association. We use a set of basic performance evaluation metrics for target association including *mostly tracked* (MT), *mostly lost* (ML), *identity switches* (IDS), *fragmentations of target trajectories* (FM), *false positives after tracking* (FPT), *false negatives after tracking* (FNT), and two CLEAR MOT metrics [36], *multi-object tracking accuracy* (MOTA) and *multi-object tracking precision* (MOTP).

The FPT metric describes the number of tracker outputs which are the false alarms, and FNT is the number of targets missed by any tracked trajectories in each frame after tracking. The IDS metric describes the number of times that the matched identity of a tracked trajectory changes, while FM is the number of times that trajectories are disconnected. Both IDS and FM metrics reflect the accuracy of tracked trajectories. The ML and MT metrics measure the percentage of tracked trajectories less than 20% and more than 80% of the time span based on the ground truth respectively.

The MOTA metric for all sequences in the benchmark is defined as [35], *i.e.*,

$$\text{MOTA} = 1 - \frac{\sum_v \sum_t (\text{FNT}_{v,t} + \text{FPT}_{v,t} + \text{IDS}_{v,t})}{\sum_v \sum_t \text{GT}_{v,t}}, \quad (1)$$

where $\text{FNT}_{v,t}$ is the false negatives after tracking, $\text{FPT}_{v,t}$ is the false positives after tracking, with the hit/miss threshold of the bounding box overlap between an output trajectory and the ground truth set to be 0.7. In addition, $\text{IDS}_{v,t}$ is the identity switches, and $\text{GT}_{v,t}$ is the number of ground truth objects at time index t of sequence v . Note that although the MOTA score is upper-bounded by 1, it can take negative values. We report the percentage MOTA $(-\infty, 100]$ in our benchmark. The MOTP metric is the average dissimilarity between all true positives and their corresponding ground truth targets, as the average overlap between all correctly matched hypotheses and their respective objects.

3.2. DETRAC MOT Metrics

The DETRAC MOT metrics considers both object detection and target association. We define the PR-MOTA curve (see Figure 5), which is a 3D curve characterizing the relation between object detection performance (precision and recall) and target association performance (MOTA). In the following, we describe the steps to create a PR-MOTA

curve⁵.

- 1) We first vary the detection threshold gradually to generate different object detections (bounding boxes) corresponding to different values of precision p and recall r . The 2D curve corresponding to (p, r) is the *precision-recall* (PR) curve \mathcal{C} that delineates the region of possible PR values of object detection.
- 2) For a particular set of object detections determined by (p, r) , we apply a target association algorithm and compute the resulting MOTA score $\Psi(p, r)$. The MOTA scores for (p, r) values on the PR curve form a 3D curve, *i.e.*, the PR-MOTA curve, as shown in Figure 5.
- 3) From the PR-MOTA curve, we calculate two DETRAC MOT metrics (Ω^*, Ψ^*) , where Ω^* is the ensemble PR-MOTA score and Ψ^* is the peak PR-MOTA score, to measure MOT performance (see Figure 5).
 - $\Psi^* = \arg \max_{\mathcal{C}} \Psi(p, r)$ is the maximal MOTA score on the PR-MOTA curve corresponding to the best performance of the MOT system.
 - $\Omega^* = \int_{\mathcal{C}} \Psi(p, r) ds$ is the line integral along the PR curve \mathcal{C} . In other words, Ω^* corresponds to the (signed) area of the curved surface formed by the PR-MOTA curve along the PR curve, as shown by the shaded area in Figure 5.

Using PR-MOTA curve and (Ω^*, Ψ^*) , we can compare different MOT algorithms by considering the effect of object detections⁶. When comparing different MOT systems, we should consider both metrics, as the Ω^* score reflects the overall performance of a MOT system, while the Ψ^* score gives the best performance of a MOT system. In the following, we evaluate different MOT systems mainly based on Ω^* . If two trackers obtain the same Ω^* , they are further ranked by Ψ^* . A method with both higher scores is considered to perform well using the DETRAC MOT metrics.

3.3. Comparison with Existing Evaluation Protocols

Evaluating the performance of MOT methods is a complex issue, the analysis in [28] has pointed out that the widely used criteria in the literature [36, 27], such as the MOTA, MOTP or IDS scores all have somewhat problems. Furthermore, there exists some issues with the associated MOT evaluation protocols. Early multi-object tracking studies [40, 3] use different object detection methods to generate inputs to different target association methods. It is known that the arbitrary choice of object detection inputs affects the MOT results. Most recent MOT evaluation works (*e.g.*, [22, 37, 26]) adopt a different protocol that uses the

⁵The PR-MOTA curve is used to compare the performance of MOT systems. Similar curves can also be created for other basic association evaluation metrics, *e.g.*, PR-MOTP, PR-IDS, PR-MT etc, which are used as the references in performance evaluation. Examples of other types of curves can be found in the supplementary materials.

⁶Notably, we have $\Psi^* \in (-\infty, 100]$ and $\Omega^* \in (-\infty, 200)$. The proofs about the range of these two metrics can be found in Appendix.

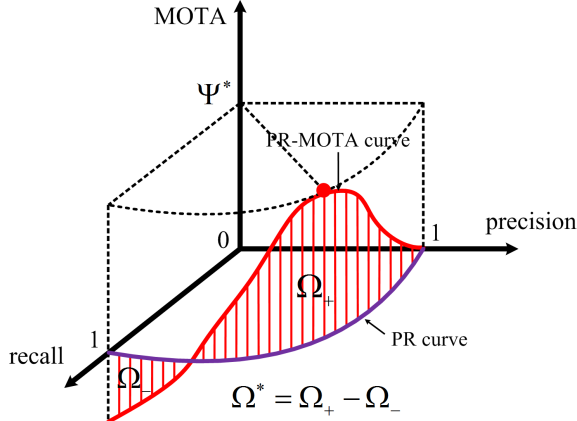


Figure 5: DETRAC MOT performance evaluation metrics Ψ^* and Ω^* : the purple curve is the precision-recall curve describing the performance of the object detection result and the red one is the PR-MOTA curve.

same fixed detection inputs to different target association methods, in order to make the MOT evaluation independent from the variations in object detection results. It has been shown [35] that the performance MOT systems cannot be reflected clearly with fixed detection inputs, and multiple synthetic detections generated by controlled noise are used for comparisons. However, these synthetically generated detection results do not fully reflect the behavior of detectors. Furthermore, in [35], the detections are randomly perturbed independently for each frame, which is different from real detectors that generate the somewhat correlated detections in consecutive frames.

In contrast, the DETRAC MOT protocol considers the detector performance for MOT evaluation. By using the 3D curves of detection (PR) and association scores (*e.g.*, MOTA, MOTP, and IDS), the DETRAC MOT protocol can better reflect the behavior of MOT systems, and is more useful for evaluating all components of a MOT system.

4. Evaluation and Analysis

4.1. Evaluation of Object Detection Methods

Object detection has gone through significant improvement in recent years, partly driven by the availability of large scale datasets and benchmarks such as the PASCAL VOC [17] and ImageNet [34]. However, the performance of four state-of-the-art object detectors on the DETRAC dataset, presented in Figure 6 with the PR curves, shows that there is still room for improvement for object detectors for real-world MOT applications. Specifically, as the PR curves in Figure 6 show, the DPM and ACF methods do not perform well on vehicle detection. The deep learning based R-CNN method performs slightly better than the ACF method. Although the most recent CompACT [8] algorithm achieves relative better performance among the four detectors, it is still far from satisfactory. In general, all the eval-

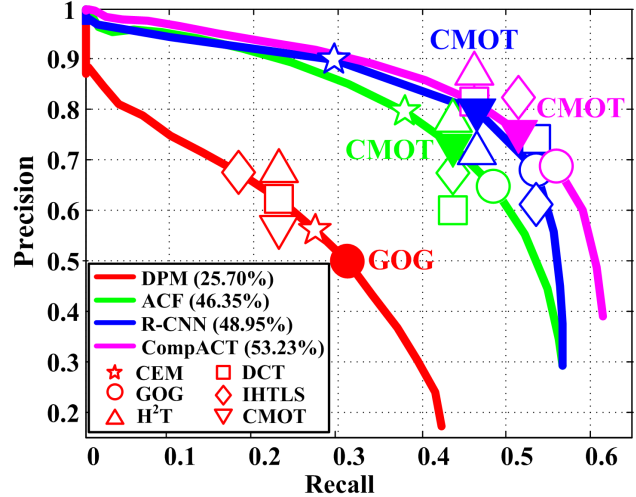


Figure 6: Performance evaluation based on combination of detection and tracking in the DETRAC benchmark. The PR curves of different object detection algorithms are assigned with different colors, and different target association algorithms are denoted by different hollow marks. Specifically, the solid marks on each PR curve represents the locations of the highest MOTA values produced by the corresponding object detection and target association algorithms. The scores in parentheses are the Average Precision (AP) using to describe the performance of object detection algorithms. This figure is better view with the electronic copy and zoomed in for details.

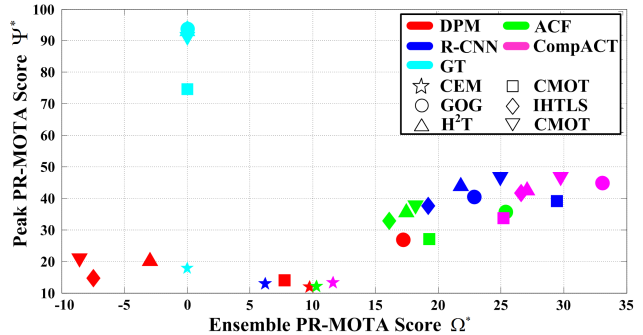
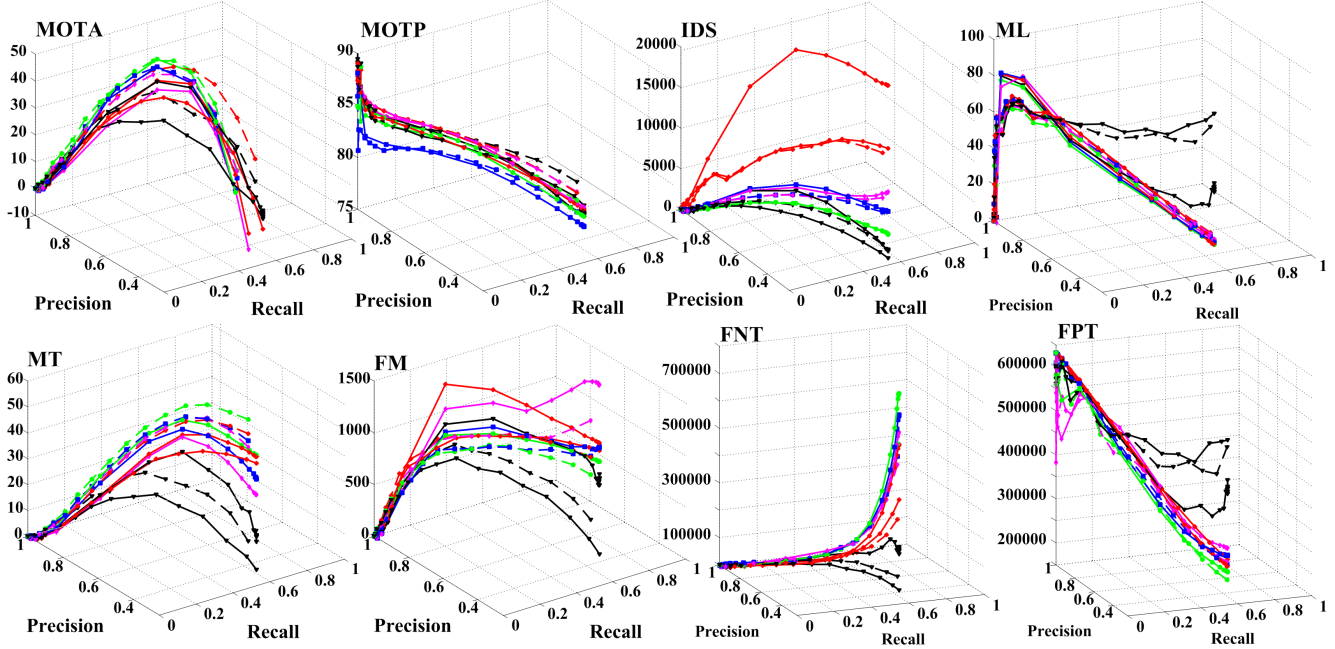


Figure 9: DETRAC MOT scores based on different combinations of four different object detection algorithms as well as the annotated ground truth and six target association algorithms. Note that since the ground truth detection does not provide a full PR-MOTA curve, we assume it correspond to a zero Ω^* score.

uated detectors have high miss rates as vehicle detection in the real scenes of the DETRAC dataset is challenging.

4.2. Evaluation of Complete MOT Systems

We use different combinations of four state-of-the-art object detection algorithms and six target association algorithms (see Table 2) for complete MOT systems, and plot the PR-MOTA, PR-MOTP, PR-MT, PR-ML, PR-IDS, PR-FM, PR-FPT and PR-FNT curves of all combinations of the object detection algorithms and target association algorithms, in Figure 7 and Figure 8 to show the tracking performance and quality of tracked trajectories in DETRAC dataset.



Method	PR-MOTA	PR-MOTP	PR-IDS	PR-MT	PR-FM	PR-ML	PR-FPT	PR-FNT
GOG-CompACT	(29.1,44.9)	(79.4,80.4)	(6694.4,9408)	(28.2,44.9)	(812.2,975)	(35.1,20.1)	(61756.5,81324)	(361104.9,257460)
CMOT-CompACT	(26.6,46.8)	(78.7,80.0)	(561.1,562)	(32.5,45.7)	(695.7,838)	(31.9,22.0)	(110670.5,80409)	(327791.1,255640)
DCT-R-CNN	(25.2,39.2)	(82.4,79.9)	(1624.8,1974)	(20.8,34.1)	(924.2,1027)	(40.6,23.6)	(70961.6,82471)	(421689.5,300290)
CMOT-R-CNN	(24.2,46.7)	(81.8,80.0)	(988.9,756)	(32.0,38.1)	(873.9,948)	(33.6,23.2)	(139603.9,53294)	(355196.4,282710)
H ² T-CompACT	(24.0,42.5)	(77.0,79.0)	(1680.9,1576)	(29.3,36.7)	(714.6,799)	(34.1,30.8)	(107811.7,46946)	(351816.1,315290)
IHTLS-CompACT	(23.7,41.7)	(78.9,80.6)	(1878.9,1825)	(28.4,40.8)	(840.5,957)	(33.5,24.8)	(103340.6,80170)	(339539.3,286830)
H ² T-R-CNN	(22.6,43.9)	(80.3,78.9)	(2986.8,3019)	(28.8,34.8)	(895.0,1012)	(35.4,24.3)	(131384.4,55519)	(377367.4,296330)
GOG-ACF	(22.4,35.7)	(81.4,80.3)	(7976.5,9863)	(24.9,35.7)	(900.2,1056)	(39.0,28.3)	(87115.5,85500)	(395455.7,311440)
DCT-CompACT	(22.3,33.6)	(79.5,81.1)	(293.4,299)	(13.9,22.0)	(585.0,730)	(52.6,45.8)	(27080.1,28216)	(435934.5,381440)
GOG-R-CNN	(22.0,40.5)	(82.7,80.0)	(16145.6,20094)	(27.4,40.8)	(1164.5,1302)	(36.1,18.1)	(107856.3,89645)	(391665.1,266180)
IHTLS-R-CNN	(18.6,37.7)	(82.5,80.0)	(3055.5,3135)	(24.5,39.9)	(1170.5,1245)	(37.8,19.6)	(128578.8,117090)	(387603.0,273930)
DCT-ACF	(17.2,27.0)	(81.6,80.8)	(231.0,246)	(10.2,17.7)	(515.1,653)	(61.0,54.1)	(26901.0,35825)	(478354.3,425550)

Figure 7: PR-MOTA, PR-MOTP, PR-IDS, PR-MT, PR-FM, PR-ML, PR-FNT, and PR-FPT curves of twelve combinations of object detection and target association algorithms achieving relative better performance based on the DETRAC MOT metrics of the PR-MOTA curve in the DETRAC benchmark, as well as the plot of the PR-MOTA scores based on all combinations of object detection and target association algorithms. The ensemble scores in the bottom right tables for other curves, *i.e.*, PR-MOTP, PR-IDS, PR-MT, PR-FM, PR-ML, PR-FNT, and PR-FPT, are similarly calculated as the ensemble PR-MOTA score Ω^* , and the peak scores for other curves are calculated at the same point on the PR curve corresponding to the peak PR-MOTA score Ψ^* . This figure is better view with the electronic copy and zoomed in for details.

From the PR-MOTA curves, we compare different MOT systems constructed by combining four state-of-the-art object detection algorithms as well as ground truth, and six state-of-the-art target association algorithms using the DETRAC MOT metrics based on Ω^* and Ψ^* of PR-MOTA curve, in the Figure 9. We observe that even though the object detection achieves perfect performance, *i.e.*, taking the annotated ground truth as input, the MOT performance is still not perfect (the optimal MOTA score is less than 95%). The results indicate that there exists a broad space for improving target association algorithms to meet real-work applications, and demonstrate that the DETRAC dataset is quite challenging for MOT.

To further evaluate the performance of different target association algorithms, we use the same object detection algorithms but varying the detection threshold to generate

the full PR-MOTA curves. Figure 10 shows the results where each plot corresponds to one object detection algorithm combined with six state-of-the-art target association algorithms. From these results, we observe:

- 1) The ranks of the target association algorithms vary as the input detection accuracy changes, *i.e.*, with different precision and recall values. For instance, as shown in the PR-MOTA curves in Figure 10, the ranks of the target association algorithms at different recall and precision values are different from each other. The results indicate that it is inadequate to use fixed object detection input (corresponding to a fixed point on the PR curve) evaluate MOT methods. The results vary significantly depending on different fixed inputs. In contrast, the DETRAC evaluation protocol is more comprehensive as it considers detection performance to evaluate MOT methods.

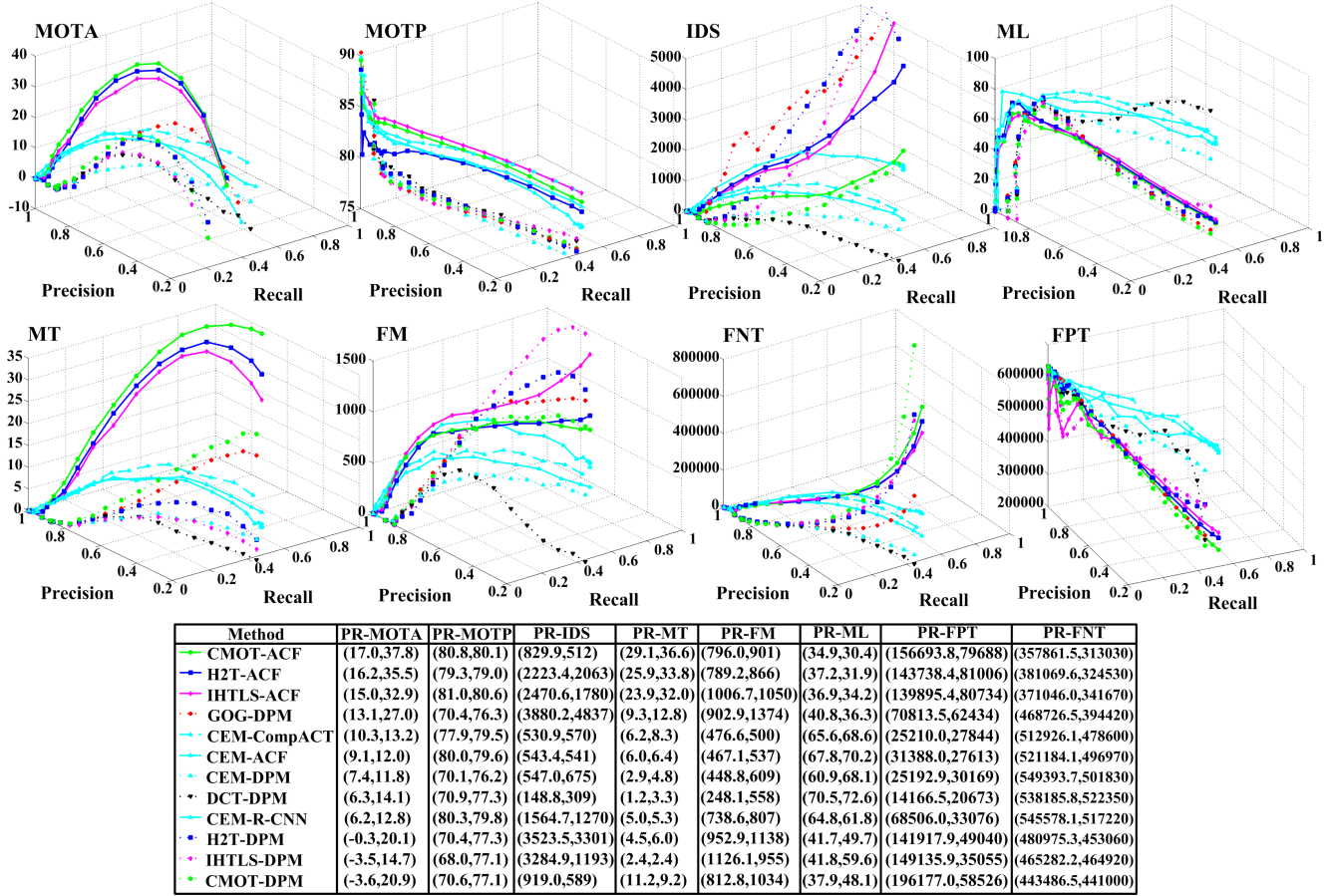


Figure 8: PR-MOTA, PR-MOTP, PR-IDS, PR-MT, PR-FM, PR-ML, PR-FNT, and PR-FPT curves of twelve combinations of object detection and target association algorithms achieving relative worse performance based on the DETRAC MOT metrics of the PR-MOTA curve in the DETRAC benchmark, as well as the plot of the PR-MOTA scores based on all combinations of input object detections (*i.e.*, four state-of-the-art detectors and ground truth) and target association algorithms. The ensemble scores in the bottom right tables for other curves, *i.e.*, PR-MOTP, PR-IDS, PR-MT, PR-FM, PR-ML, PR-FNT, and PR-FPT, are similarly calculated as the ensemble PR-MOTA score Ψ^* , and the peak scores for other curves are calculated at the same point on the PR curve corresponding to the peak PR-MOTA score Ψ^* . This figure is better view with the electronic copy and zoomed in for details.

2) For different object detection algorithms, the best MOT performance is achieved by combining different target association algorithms. For instance, the GOG tracker achieves the best performance with the DPM algorithm, while the CMOT target association approach achieves the best performance with the ACF, R-CNN and CampACT object detection schemes. This observation shows that optimal MOT performance is achieved when different object detection algorithms are properly combined with target association methods.

Furthermore, we plot the best performance point, *i.e.*, the best MOTA score Ψ^* point, of each target association algorithm on the PR curves generated by different object detection methods in Figure 6. We find that the best MOT performance is usually achieved with high precision (large than 0.5) and moderate recall scores (between 0.2 and 0.6) of the object detections, which shows that target association methods are more sensitive to false positives than false negatives.

That may be explained by that the target association algorithms are able to recover the false negatives according to the correct cross-frame associations, but not able to differentiate true from false positives. In practical applications, there is a tradeoff between precision and recall. This observation implies that to achieve better MOT performance, we can use an object detection method that generates fewer false positives, even if it produces more false negatives at the same time.

4.3. Run Time

Since different object detection algorithms requires different platform for evaluation, *e.g.*, the R-CNN method [21] requires the GPU for both training and testing, while a CPU desktop is enough for the ACF method [13], we only report the run-time speed of all the evaluated target association algorithms. That is, for each target association algorithm, given the input detection produced by different de-

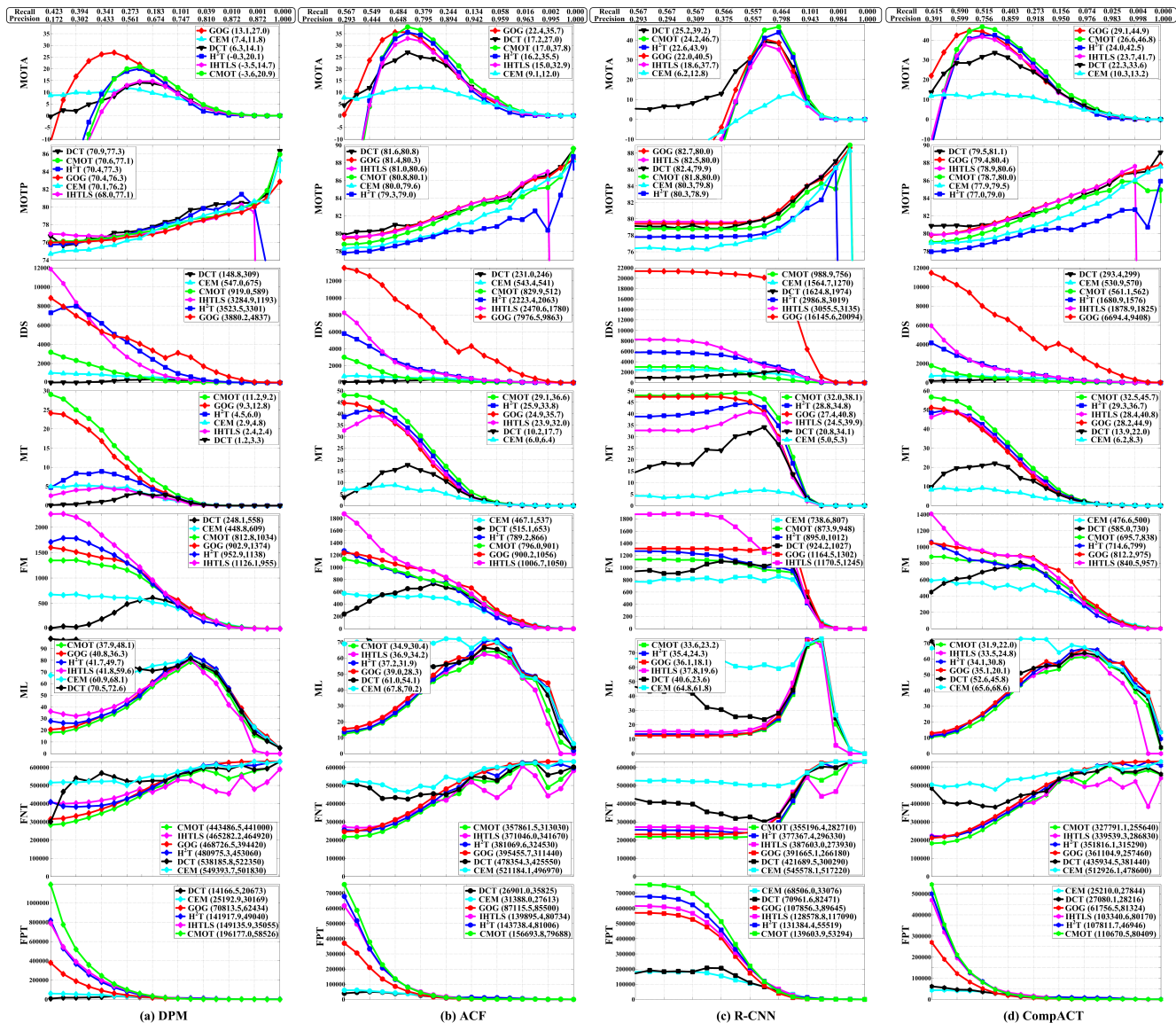


Figure 10: Performance curves based on eight basic metrics, *i.e.*, MOTA, MOTP, IDS, MT, FM, ML, FNT, and FPT, of different association methods with the same object detection algorithms in the DETRAC benchmark. This figure is better view with the electronic copy and zoomed in for details.

tection algorithms, *i.e.*, DPM [18], ACF [13], R-CNN [21], and CompACT [8], with the largest F-score, the average execution speeds on 40 sequences in DETRAC-test set of all trackers are presented in Table 3. We run all the target association methods on a laptop with a 2.9 GHz Intel i7 processor and 16 GB memory. Frame-per-second (fps) is used to measure the speed of the tracker.

5. Conclusions

In this work, we present a large scale multi-object tracking benchmark (DETRAC) consisting of 100 video sequences with target-level, frame-level and sequence-level annotations. We perform comprehensive experiments to

Table 3: Average run-time speed of the target association algorithms on the video sequences of DETRAC-test set with the largest F-score detection responses produced by four different detection algorithms, *i.e.*, DPM [18], ACF [13], R-CNN [21], and CompACT [8].

Trackers	Codes	DPM	ACF	R-CNN	CompACT	Average
CEM [2]	Matlab	4.49	3.74	5.40	4.62	4.56
GOG [33]	Matlab	476.52	319.29	352.80	389.51	384.53
DCT [3]	Matlab,C++	2.85	1.29	0.71	2.19	1.76
IHTLS [12]	Matlab	7.94	5.09	11.96	19.79	11.20
H ² T [37]	C++	1.77	1.08	2.78	3.02	2.16
CMOT [4]	Matlab	4.48	3.12	3.59	3.79	3.75

benchmark the performance of four object detection and six target association methods. This large scale benchmark en-

ables us to perform a study of the effect of detection accuracy to MOT performance, which has not been explored extensively in previous benchmark studies of MOT methods.

Based on our study, there are several aspects that a practitioner should consider when building MOT systems to achieve satisfactory performance while keeping the runtime efficiency. First, we should consider object detection and target association jointly to evaluate performance of MOT systems. We suggest using the DETRAC MOT protocol for this purpose. Second, the DETRAC MOT metrics Ω^* and Ψ^* can better reflect the overall MOT system performance. Third, our results suggest that many MOT methods are relative robust to false negatives and sensitive to false positives.

In the further, we would like to enlarge the DETRAC benchmark dataset, potentially by including video sequences and annotations for pedestrians, and focus on theoretical analysis of the DETRAC MOT metrics, so as to better understand the MOT systems.

References

- [1] M. Andriluka, S. Roth, and B. Schiele. People-tracking-by-detection and people-detection-by-tracking. In *CVPR*, 2008.
- [2] A. Andriyenko and K. Schindler. Multi-target tracking by continuous energy minimization. In *CVPR*, pages 1265–1272, 2011.
- [3] A. Andriyenko, K. Schindler, and S. Roth. Discrete-continuous optimization for multi-target tracking. In *CVPR*, pages 1926–1933, 2012.
- [4] S. H. Bae and K. Yoon. Robust online multi-object tracking based on tracklet confidence and online discriminative appearance learning. In *CVPR*, pages 1218–1225, 2014.
- [5] F. Bashir and F. Porikli. Performance evaluation of object detection and tracking systems. In *PETS*, 2006.
- [6] B. Benfold and I. Reid. Stable multi-target tracking in real-time surveillance video. In *CVPR*, pages 3457–3464, 2011.
- [7] M. D. Breitenstein, F. Reichlin, B. Leibe, E. Koller-Meier, and L. J. V. Gool. Online multi-person tracking-by-detection from a single, uncalibrated camera. *TPAMI*, 33(9):1820–1833, 2011.
- [8] Z. Cai, M. Saberian, and N. Vasconcelos. Learning complexity-aware cascades for deep pedestrian detection. In *ICCV*, 2015.
- [9] R. Collins, X. Zhou, and S. K. Teh. An open source tracking testbed and evaluation web site. In *PETS*, 2005.
- [10] N. Dalal and B. Triggs. Histograms of oriented gradients for human detection. In *CVPR*, pages 886–893, 2005.
- [11] A. Dehghan, S. M. Assari, and M. Shah. GMMCP-Tracker: globally optimal generalized maximum multi clique problem for multiple object tracking. In *CVPR*, 2015.
- [12] C. Dicle, O. I. Camps, and M. Szaier. The way they move: Tracking multiple targets with similar appearance. In *ICCV*, pages 2304–2311, 2013.
- [13] P. Dollár, R. Appel, S. Belongie, and P. Perona. Fast feature pyramids for object detection. *TPAMI*, 36(8):1532–1545, 2014.
- [14] P. Dollár, C. Wojek, B. Schiele, and P. Perona. Pedestrian detection: An evaluation of the state of the art. *TPAMI*, 34(4):743–761, 2012.
- [15] M. Enzweiler and D. M. Gavrila. Monocular pedestrian detection: Survey and experiments. *TPAMI*, 31(12):2179–2195, 2009.
- [16] A. Ess, B. Leibe, and L. J. V. Gool. Depth and appearance for mobile scene analysis. In *ICCV*, pages 1–8, 2007.
- [17] M. Everingham, S. M. A. Eslami, L. V. Gool, C. K. I. Williams, J. M. Winn, and A. Zisserman. The pascal visual object classes challenge: A retrospective. *IJCV*, 111(1):98–136, 2015.
- [18] P. F. Felzenszwalb, R. B. Girshick, D. A. McAllester, and D. Ramanan. Object detection with discriminatively trained part-based models. *TPAMI*, 32(9):1627–1645, 2010.
- [19] J. M. Ferryman and A. Shahroki. PETS2009: dataset and challenge. In *AVSS*, pages 1–6, 2009.
- [20] A. Geiger, P. Lenz, and R. Urtasun. Are we ready for autonomous driving? the KITTI vision benchmark suite. In *CVPR*, pages 3354–3361, 2012.
- [21] R. B. Girshick, J. Donahue, T. Darrell, and J. Malik. Rich feature hierarchies for accurate object detection and semantic segmentation. In *CVPR*, pages 580–587, 2014.
- [22] C. Huang, Y. Li, and R. Nevatia. Multiple target tracking by learning-based hierarchical association of detection responses. *TPAMI*, 35(4):898–910, 2013.
- [23] S. Hwang, J. Park, N. Kim, Y. Choi, and I. S. Kweon. Multispectral pedestrian detection: Benchmark dataset and baseline. In *CVPR*, 2015.
- [24] H. Izadinia, I. Saleemi, W. Li, and M. Shah. (MP)²T: Multiple people multiple parts tracker. In *ECCV*, pages 100–114, 2012.
- [25] A. Krizhevsky, I. Sutskever, and G. E. Hinton. Imagenet classification with deep convolutional neural networks. In *NIPS*, pages 1106–1114, 2012.
- [26] L. Leal-Taixé, A. Milan, I. D. Reid, S. Roth, and K. Schindler. Motchallenge 2015: Towards a benchmark for multi-target tracking. *arXiv preprint*, abs/1504.01942, 2015.
- [27] Y. Li, C. Huang, and R. Nevatia. Learning to associate: Hybridboosted multi-target tracker for crowded scene. In *CVPR*, pages 2953–2960, 2009.
- [28] A. Milan, K. Schindler, and S. Roth. Challenges of ground truth evaluation of multi-target tracking. In *CVPR Workshops*, pages 735–742, 2013.
- [29] A. Milan, K. Schindler, and S. Roth. Detection- and trajectory-level exclusion in multiple object tracking. In *CVPR*, pages 3682–3689, 2013.
- [30] W. Ouyang and X. Wang. A discriminative deep model for pedestrian detection with occlusion handling. In *CVPR*, pages 3258–3265, 2012.
- [31] G. Overett, L. Petersson, N. Brewer, L. Andersson, and N. Petterson. A new pedestrian dataset for supervised learning. In *TIIVS*, pages 373–378, 2008.

- [32] C. Papageorgiou and T. Poggio. A trainable system for object detection. *IJCV*, 38(1):15–33, 2000.
- [33] H. Pirsiavash, D. Ramanan, and C. C. Fowlkes. Globally-optimal greedy algorithms for tracking a variable number of objects. In *CVPR*, pages 1201–1208, 2011.
- [34] O. Russakovsky, J. Deng, H. Su, J. Krause, S. Satheesh, S. Ma, Z. Huang, A. Karpathy, A. Khosla, M. Bernstein, A. C. Berg, and L. Fei-Fei. ImageNet Large Scale Visual Recognition Challenge. *IJCV*, pages 1–42, april 2015.
- [35] F. Solera, S. Calderara, and R. Cucchiara. Towards the evaluation of reproducible robustness in tracking-by-detection. In *AVSS*, 2015.
- [36] R. Stiefelhagen, K. Bernardin, R. Bowers, J. S. Garofolo, D. Mostefa, and P. Soundararajan. The clear 2006 evaluation. In *CLEAR*, pages 1–44, 2006.
- [37] L. Wen, W. Li, Z. Lei, D. Yi, and S. Z. Li. Multiple target tracking based on undirected hierarchical relation hypergraph. In *CVPR*, pages 3457–3464, 2014.
- [38] Z. Wu, N. W. Fuller, D. H. Theriault, and M. Betke. A thermal infrared video benchmark for visual analysis. In *CVPRWorkshops*, pages 201–208, 2014.
- [39] B. Yang and R. Nevatia. Online learned discriminative part-based appearance models for multi-human tracking. In *ECCV*, pages 484–498, 2012.
- [40] A. R. Zamir, A. Dehghan, and M. Shah. GMCP-Tracker: Global multi-object tracking using generalized minimum clique graphs. In *ECCV*, pages 343–356, 2012.
- [41] L. Zhang, Y. Li, and R. Nevatia. Global data association for multi-object tracking using network flows. In *CVPR*, 2008.

Appendix

We give the proofs about the range of two DETRAC MOT metrics, *i.e.*, peak PR-MOTA metric Ψ^* and ensemble PR-MOTA metric Ω^* .

Peak PR-MOTA metric. Since the MOTA score $\Psi(p, r) \in (-\infty, 100]$, we have the Peak PR-MOTA metric $\Psi^* = \arg \max_{\mathcal{C}} \Psi(p, r) \in (-\infty, 100]$.

Ensemble PR-MOTA metric. The ensemble PR-MOTA metric Ω^* is defined as the line integral along the PR curve, *i.e.*,

$$\Omega^* = \int_{\mathcal{C}} \Psi(p, r) ds \quad (2)$$

where \mathcal{C} is the PR curve, and $\Psi(p, r)$ is the MOTA value corresponding to the precision p and recall r on the PR curve. Since any MOTA score $\Psi(p, r) \in (-\infty, 100]$, we have the lower bound of Ω^* is $-\infty$. We present the upper bound of Ω^* as follows. Let $\mathcal{C}_0, \dots, \mathcal{C}_n$ be the dividing points on the PR curve, where the i -th point is $\mathcal{C}_i = (p_i, r_i)$ corresponding to the precision p_i and recall r_i on the PR curve, and \mathcal{C}_0 and \mathcal{C}_n are two end points of the PR curve. We denote the length of the i -th arc determined by $\mathcal{C}_{i-1}\mathcal{C}_i$ is Δs_i . Thus, we have $\Delta s_i = \sqrt{\Delta p_i^2 + \Delta r_i^2}$. Let

$\lambda = \max_{1 \leq i \leq n} \Delta s_i$. Then, the ensemble PR-MOTA metric Ω^* can be represented as

$$\Omega^* = \int_{\mathcal{C}} \Psi(p, r) ds = \lim_{\lambda \rightarrow 0} \sum_{i=1}^n \Psi(p_i, r_i) \Delta s_i \quad (3)$$

$\forall i$, we have $\Psi(p_i, r_i) \leq 100$. Thus, we have

$$\begin{aligned} \Omega^* &\leq 100 \cdot \lim_{\lambda \rightarrow 0} \sum_{i=1}^n \Delta s_i \\ &= 100 \cdot \lim_{\lambda \rightarrow 0} \sum_{i=1}^n \sqrt{\Delta p_i^2 + \Delta r_i^2} \\ &\leq 100 \cdot \lim_{\lambda \rightarrow 0} \sum_{i=1}^n (|\Delta p_i| + |\Delta r_i|) \\ &= 100 \cdot \lim_{\lambda \rightarrow 0} \left(\sum_{i=1}^n |\Delta p_i| + \sum_{i=1}^n |\Delta r_i| \right) \end{aligned}$$

Since the precision p and recall r on the PR curve are in the interval $[0, 1]$, *i.e.*, $p \in [0, 1]$ and $r \in [0, 1]$, we have $\sum_{i=1}^n |\Delta p_i| = 1$ and $\sum_{i=1}^n |\Delta r_i| = 1$. In this way, we obtain $\Omega^* \leq 200$. The equal sign is achieved under two constraints, *i.e.*, (1) precision $p \neq 0$, recall $r = 0$, and recall $r \neq 0$, precision $p = 0$; (2) For any precision p and recall r values of the input detection, the target association method can always achieve the best MOTA score 100. The two constraints are the idea cases, which are impractical in real applications. Thus, we have $\Omega^* \in (-\infty, 200)$.